Acta Oceanol. Sin., 2015, Vol. 34, No. 7, P. 19–31
DOI: 10.1007/s13131-015-0657-0
http://www.hyxb.org.cn
E-mail: hyxbe@263.net

The Beaufort Gyre variation and its impacts on the Canada Basin in 2003–2012

ZHONG Wenli[1]*, ZHAO Jinping[1], SHI Jiuxin[1], CAO Yong[1]

[1] Key Laboratory of Physical Oceanography, Ocean University of China, Qingdao 266100, China

Received 20 June 2014; accepted 3 Februbary 2015

Abstract

The Beaufort Gyre (BG) was spun up in the last decade which is an important factor in regulating the variation of the upper ocean. The heat content and freshwater content of the upper ocean increased gradually in the Canada Basin, as did momentum input. Both the geostrophic wind curl and freshwater content could contribute to the spin-up of BG. However, even though there is no change of the wind field the increasing freshwater alone could result in the spin-up of BG. In this study we show that the Pacific Water is difficult to flow into the central basin as the BG spins up and the maximum temperature of the Pacific Summer Water (PSW) experienced a dramatic decrease inside the BG in 2005 and 2009 due to a change of flow pathway of PSW. The enhancement of Ekman Pumping (EP) contributed to the deepening of the Pacific Winter Water by piling up more freshwater. This change of water column dynamics has also contributed to the deepening ofthe Atlantic Water core after 2007. The EP decreased significantly in 2012 (indicating a spin down of BG) and the direction of Ekman transport turned to the north, which favoured the release of freshwater that had resided in the basin for years.

Key words: Beaufort Gyre, Ekman pumping, freshwater content, geostrophic current, Canada Basin

Citation: Zhong Wenli, Zhao Jinping, Shi Jiuxin, Cao Yong. 2015. The Beaufort Gyre variation and its impacts on the Canada Basin in 2003–2012. Acta Oceanologica Sinica, 34(7): 19–31, doi: 10.1007/s13131-015-0657-0

1 Introduction

As one of the important components of the large scale circulation in the Arctic Ocean, the Beaufort Gyre (BG) plays a crucial role in regulating the Arctic climate (Proshutinsky and Johnson, 1997; Asplin et al., 2009; Proshutinsky et al., 2009). Under the influence of prevailing Beaufort Sea high, the typical feature of BG is an anticyclonic circulation. The upper ocean water and sea ice would converge on the anticyclonic BG center, which results in the largest freshwater reservoir (45 000 km^3) in the Arctic Ocean (Aagaard and Carmack, 1989). The reservoir is 10–15 times larger than the annual river runoff volume and at least two times larger than the freshwater stored in the Arctic sea ice (Proshutinsky et al., 2002). The distribution and outflow of freshwater are affected by the intensity of BG. The recede of BG or even reversal would result in freshwater releasing into the North Atlantic Ocean, which further caused the salinity anomaly there (one from 1968 to 1978, one in the 1980s and one in the 1990s) and may potentially affect the formation of deep water and the climate change (Aagaard et al., 1985; Dickson et al., 1988; Rennermalm et al., 2006).

The Arctic Ocean is regulated by two phases of multi-decadal variability of Low Frequency Oscillation (LFO) with lower/higher than normal sea level pressure (SLP) and cyclonic/anticyclonic circulation regime while the BG retreated/intensified and the exports of more/less sea ice in positive/negative phase (Polyakov et al., 2004).

The Arctic Ocean was dominated by the anticyclonic circulation regime in the last decade (McPhee et al., 2009; Proshutinsky et al., 2013; Giles et al., 2012) while the sea ice was experiencing an inevitable decline. One of the factors causing the retreat of sea ice is the air temperature increasing which further makes the AO (Arctic Oscillation) regulating mechanism in variation of sea ice become less obvious (Thompson and Wallace, 1998; Comiso et al., 2008). There is evidence that the property of AO has changed (Wang et al., 2009; Overland and Wang, 2010). What's more, the AO only explains 50% variability of SLP (Rigor et al., 2002). It does not necessarily describes the variations in the wind (which is related to the gradient of SLP) or in the stress curlin the BG (Yang and Proshutinsky, 2013). After analyzing the simulated annual sea ice motion and ocean circulation in the Arctic Ocean, Proshutinsky and Johnson (1997) proposed the Arctic Ocean Oscillation (AOO) index which could better represent the circulation regime that dominates the Arctic Ocean. AOO relates not only the atmospheric forcing but also the ocean configuration (bathymetry and coastline), sea ice condition and the impact of river runoff. The Arctic Ocean is dominated by the anticyclonic circulation regime from 1997 to 2013 as the BG had been intensified (Proshutinsky et al., 2013).

The water column properties in the Canada Basin are unique under the influence of BG. The isopycnal appears as a bowl shape with the deepest inside of the BG and the shallowest outside of BG (Proshutinsky et al., 2002). Within the anticyclonic BG, the upper ocean is converged by the Ekman Pumping (EP) that changes the properties of water column. Dynamic height calculation shows that the impact of BG could reach the depth of Atlantic Water (AW) (McLaughlin et al., 2009). In the last decade,

Foundation item: The Key Project of Chinese Natural Science Foundation under contract No. 41330960; the National Basic Research Program of China under contract No. 2015CB953902; the Project of Study on the seasonal halocline and near sea surface temperature maximum in Arctic under contract No. 41306196.

*Corresponding author, E-mail: wlzhongouc@163.com

the strength of BG shows an increasing trend (Proshutinsky et al., 2009; McLaughlin and Carmack, 2010; Gile et al., 2012; McPhee, 2013). The mechanism of BG spin-up is attributed to the retreat of sea ice that enhanced the sea ice motion and the increased air-ice and ice-ocean drag coefficients caused by higher ice roughness (Giles et al., 2012; Tsamados et al., 2014). The spin-up of BG can deepen the Pacific summer water (PSW) because the EP can converge freshwater to the BG interior and resulted in desalination in some water masses, such as the near surface temperature maximum (NSTM) and remnant of the previous winter mixed layer (WML) (Jackson et al., 2011). The increasing freshwater content in the Pacific Water layers from 2005 to 2008 in the Canada Basin was due to a circulation pattern that fresh shelf water was carried from the Eurasian side eastward along the Russian coast into the Canada Basin that characterized by an increased AO Index (Morison et al., 2012). Timmermans et al. (2014) pointed out the PSW at the surface in the Chukchi Sea propagates to the interior Canada Basin through subduction along the isopycnals that outcrop in the Chukchi Sea which emphasized the importance of Ekman transport convergence.Recent study shows that although the AW remains relatively warm inside the BG, the AW deepened as the BG spin-up. This indicates that the dynamic effect of BG has overwhelmed the thermodynamic effect of AW after 2007 (Zhong and Zhao, 2014).

Mainly based on the hydrographic data obtained from 2003 to 2012, we analyzed the variation of BG and its impacts on the Canada Basin. Section 2 describes our method and data that used in this study. In Section 3, we give a definition of BG and use the Ekman pumping to indicate the strength of BG. Then we discuss the variation of geostrophic wind curl in maintaining the BG. Section 4 shows the impacts of BG on the Canada Basin. Section 5 summarizes the study.

2 Data and method

The hydrographic data that used in this study are obtained from the Beaufort Gyre Exploration Project (BGEP), the Japan Agency for Marine–Earth Science and Technology (JAMSTEC), the Chinese Arctic Research Expedition (CHINARE), the Western Arctic Shelf Basin Interactions Project (SBI) and the Swedish Icebreaker Oden (ODEN). The Ice Tether Profilers (ITP) data (ITP number 1–6, 8, 11, 13, 18, 21–22, 32–33, 35, 39, 41–42) are also used here. These ITP buoys provided two profiles or four profiles of conductivity-temperature-depth (CTD) in a day in the upper 800 m of the Canada Basin. We interpolated the data to 1db to have the same resolution as ship base CTD cast profiles. All the ship base hydrographic survey was carried out in the time range of late July to early October that could represent the summer of the Canada Basin. ITP data in the time range between July 20 and October 10 were chosen for analysis. Table 1 shows the details of all data set. The Gaussian interpolation formula was used to interpolate all the CTD data. The influence radius was chosen as 300 km (details refer to Appendix).

Table 1. The hydrographic data that used in this study are listed below and references for additional information about instruments and their accuracies

Data set	Year	Month	Reference	Source URL
BGEP	2003–2012	7–10	McLaughlin et al. (2008)	http://www.whoi.edu/beaufortgyre/
JAMSTEC	2004, 2008, 2009	9–10	Shimada et al. (2004)	http://www.godac.jamstec.go.jp/darwin/
CHINARE	2008, 2010	7–9	Zhong and Zhao (2014)	http://www.chinare.org.cn
SBI	2003	7–8	Swift and Codispoti (2003)	http://www.eol.ucar.edu/projects/sbi/ctd.shtml
ODEN	2005	8–9	Karlqvist (2005)	http://cchdo.ucsd.edu/
ITP	2004–2012	7–10	Proshutinsky et al. (2009)	http://www.whoi.edu/itp

The sea ice concentration data set was derived using measurements from the Scanning Multichannel Microwave Radiometer (SMMR) on the Nimbus–7 satellite and from the Special Sensor Microwave/Imager (SSM/I) sensors on the Defense Meteorological Satellite Program's (DMSP) –F8, –F11, and –F13 satellites, which havea grid size of 25 km×25 km (Comiso, 2000). The data is available at http://nsidc.org/data/nsidc-0079.

Daily-mean sea level pressure over the Arctic Ocean was derived from the National Center for Environmental Prediction/National Center for Atmospheric Research (NCEP/NCAR) reanalysis data set (Kalnay et al., 1996). The horizontal resolution of the data is 2.5°×2.5°. The data are available at http://www.esrl.noaa.gov/psd/data/gridded/. Daily sea ice motion data was derived from the Polar Pathfinder Daily 25 km EASE-Grid Sea Ice Motion Vectors (Fowler et al., 2013) for the period from 1978 to 2012 with a resolution of 25 km. The data are available at http://nsidc.org/data/nsidc-0116.html.

The surface stress over the sea-ice covered ocean was calculated based on the sea ice motion data. Using the wind stress and ice-ocean stress we then calculated the total stress on each grid based on the sea ice concentration as suggested by Yang (2009). Daily Ekman Pumping was calculated based on the total stress and then was averaged to obtain the monthly mean fields; the latter are used for analysis. All the primary data were interpolated on the EASE-grid with a resolution of 25 km.

3 The variation of Beaufort Gyre

3.1 *The Beaufort Gyre domain*

Figure 1 shows an anticyclonic circulation known as the oceanic Beaufort Gyre circulation that dominates in the Canada Basin with its center at 72°N, 150°W (Fig. 1). One of the factors that control the strength of BG is the variation of freshwater content in the BG domain (e.g., McPhee, 2013).

We adopted a method similar to Jackson et al. (2011) to determine the center of BG. The basic idea is that we at first try to find the minimum salinity at 40 m (the depth influenced by BG directly) and then use this salinity to determine the depth of isohaline for each year (due to the fresher trend in the upper ocean, same isohaline could not be used for comparison purpose). The depth of isohaline is divided into three regions, inside of BG (25–40 m), the transition zone (16–24 m) and outside of BG (0–15 m). The region inside the BG occupied a large scope in most of the eastern basin in 2003, in southeastern basin in 2004 and 2006, in the south-central basin in 2005, in the east-central basin in 2007, in the southern basin in 2008, in the southwestern basin in

2009, 2011 and 2012, in the west-central basin in 2010 (Fig. 2). It seems that the BG center is shifting toward the southwestern basin. We should note that the hydrographic data were not obtained synchronously, the BG region we got here is just a snapshot of the ocean. In addition, the difference of surface stress between the sea ice cover region and ice-free region may result in oval shape of BG. The BG region is not synchronized with the SLP which indicates the oceanic adjustment is lag behind the atmospheric variation. In summer when the wind become weaker or it may even reverse to cyclonic, the ocean geostrophic circulation will prevail and drive the sea ice motion against the wind (Proshutinsky et al., 2002).

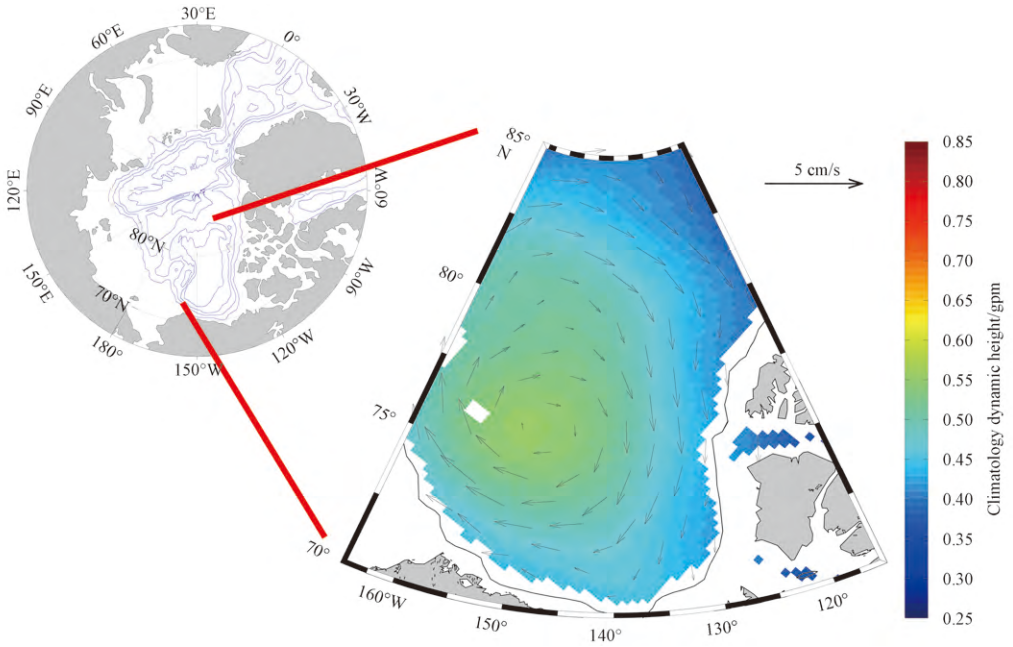

Fig. 1. The climatology dynamic height (the unit in color bar is gpm, i.e., the geopotential meter) and the surface geostrophic current in the Canada Basin (relative to 400×10^4 Pa). The thin black line shows the 400 m isobaths. Data are from the Polar Science Center Hydrographic Climatology (PHC).

3.2 *The strength of Beaufort Gyre*

The strength of BG can be depicted by the change of dynamic height (McLaughlin et al., 2011), the surface geostrophic current (McPhee, 2013), the surface stress curl (Tsamados et al., 2014; Zhong and Zhao, 2014) and the Ekman Pumping (EP).

Here we calculate the Ekman Pumping to study the strength of BG. The EP converged the surface water in the Canada Basin that resulted in downwelling inside the basin and upwelling in the continental slope region (Fig. 3a). The Ekman Pumping was weak in 2003, 2006 and 2012 with less than 2 cm/d in the BG region and upwelling prevailed in the basin for these years. In the other years during the period of 2003–2012, there is a maximum downwelling in the southwestern basin which was corresponding to the convergence center of surface water. The EP reaches the strongest in 2005, 2007–2010 (especially in 2007 larger than 4 cm/d) and the weakest in 2006 and 2012. The most obvious change in 2012 was the northward Ekman transport that induced the strong upwelling in the southern Beaufort Sea. The northward Ekman transport favours the release of freshwater that used to reside in the Canada Basin for years (Proshutinsky et al., 2009; Giles et al., 2012; de Steur, et al., 2013; Curry et al., 2014). The surface freshening in the Eurasian Basin in 2010 is believed to be caused by the release of freshwater as the BG became weaker (Timmermans et al., 2011). The EP showed a positive trend in 1995–2012 with an annual mean increase of 0.11 cm/d and the mean Ekman Pumping velocity was –1.35 cm/d during 1995–2002 and –2.52 cm/d during 2003–2012 (Fig. 3b). The surface stress curl in the Beaufort Sea was more negative (or greater Ekman pumping) in 2000s than previous 5 decades even though the meanSLP was significantly higher (Yang and Proshutinsky, 2013). The EP is strongly influenced by the oceanic and sea-ice processes.

3.3 *Impact of the geostrophic wind curl on the Beaufort Gyre*

The Beaufort Sea high (BSH) plays an important role in forcing the BG. The BSH shows a great variation between months with its climatology center in the Canada Basin (Moore, 2012). Here we inspect the geostrophic wind curl in the BG area whose variation could be divided into two period: 1995–2002 with the mean geostrophic wind curl 5.16×10^{-6} m/s^2 and 2003–2012 with the mean geostrophic wind curl -4.13×10^{-6} m/s^2 (Fig. 4). The negative geostrophic wind curl enhanced in 2003–2012 may be one of the triggers responsible for the increasing Ekman Pumping. However, changes in ice dynamics (thinner and less areal coverage) may be the main reason for the increasing surface stress curl thus the increasing Ekman Pumping (Rampal et al., 2009; Yang, 2009). Except for the strongest geostrophic wind in 2007, there is no obvious trend for the variation of geostrophic wind curl in 2003–2012. The steep temperature gradient between the summer sea ice and ice-free area may be responsible for the anomalously strong geostrophic wind in 2007 and some special synoptic type (Synoptic-scale atmospheric circulation patterns, are classified from daily mean sea level pressure data) (Asplin et al., 2009). We should notice that not only the sea ice motion and wind provide a negative vorticity in maintaining the BG, but also the volume flux of the Pacific winter water (Itoh et al., 2012).

4 The impact of Beaufort Gyre on the water column in the Canada Basin

4.1 *Impact of BG on the upper ocean*

The spin-up of BG would converge more freshwater in the Canada Basin. The freshwater in the Canada Basin shows a dramatic increase in 2000s (McPhee et al., 2009; Proshutinsky et al., 2009; Rabe et al., 2014; Morison et al., 2012). The freshwater content was relatively stable in 2003–2006 with the highest value (22 m) center at the southern basin (Fig. 5). The center of freshwater content is moving toward the southwestern basin with the highest value larger than 28 m after 2007. The freshwater increase had persisted until 2010 and then it gradually decreased. The retreat of sea ice and increase of river runoff all contributed to the freshwater content. The river runoff showed a great variability in the southern basin with no obvious trend, while river runoff component of freshwater content showed an increasing trend of 0.7 m/a in the central basin during 2003–2007 (Yamamoto-Kawai et al., 2009). From 2003 to 2011 this freshwater content had increased by more than 5 000 km^3 while river discharge increased for this time is less than (100±100) km^3 (Andrey Proshutinsky, by personal communication). Three factors contribute to the increasing freshwater content: the spin-up of BG, more sea ice melt-water and river runoff. The impact of EP was not obvious before 2007 when there were large areas of sea ice cover while after 2007 the convergence and increase of freshwater were controlled by stronger EP. The EP (annual mean, figures not shown here) decreased year by year in the BG region after 2010 which was responsible for the decreasing freshwater content in the Canada Basin after 2010.

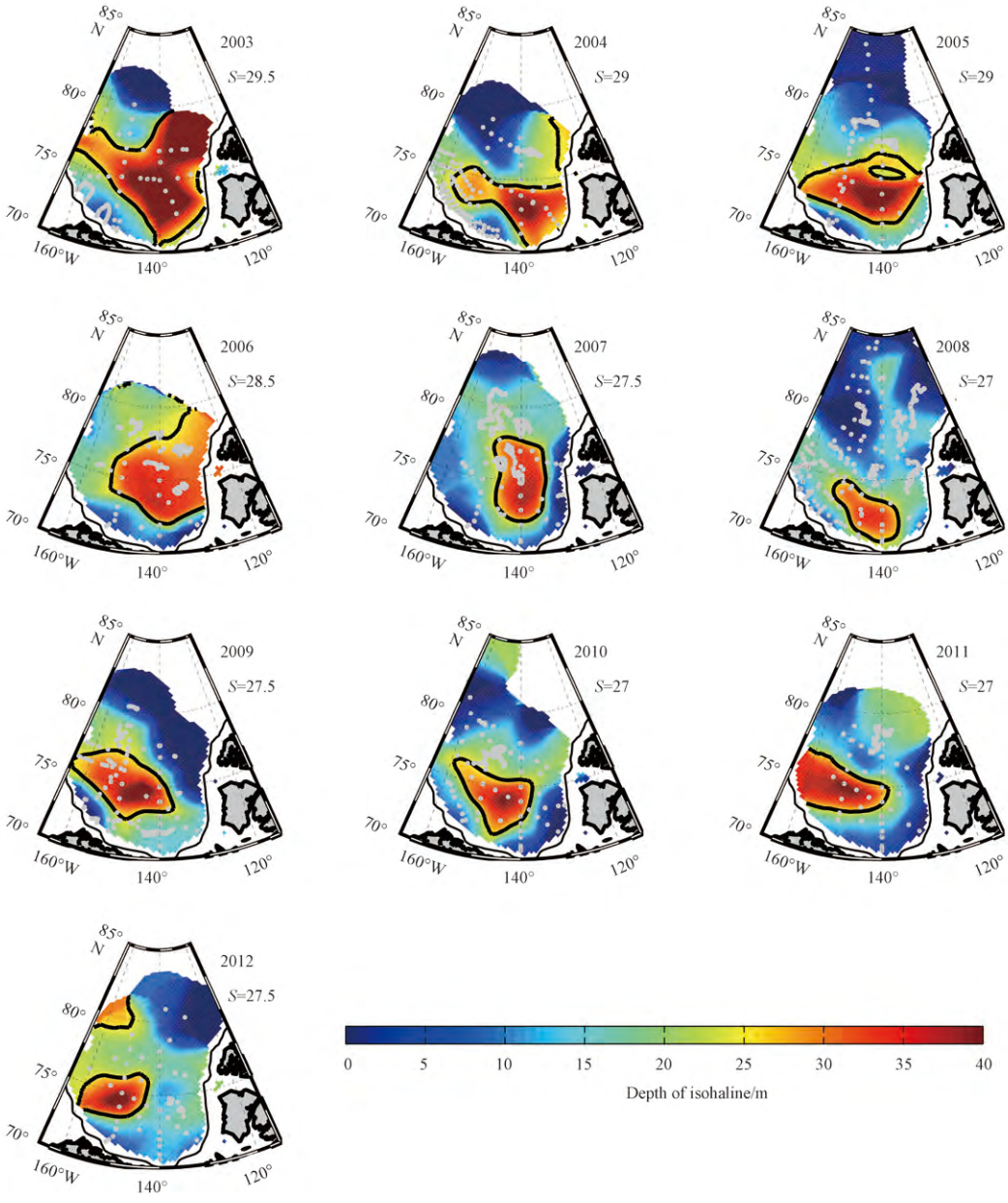

Fig. 2. Depth of the chosen isohaline (shown as the "*S*" value, "*S*" represents the salinity) for each year. The region inside the Beaufort Gyre is circled by 25 m isoline, shown as the thick black line. The gray dots indicate the locations where the CTD data were collected, and the values between stations are interpolated. The thin black lines represent the 400 m isobaths.

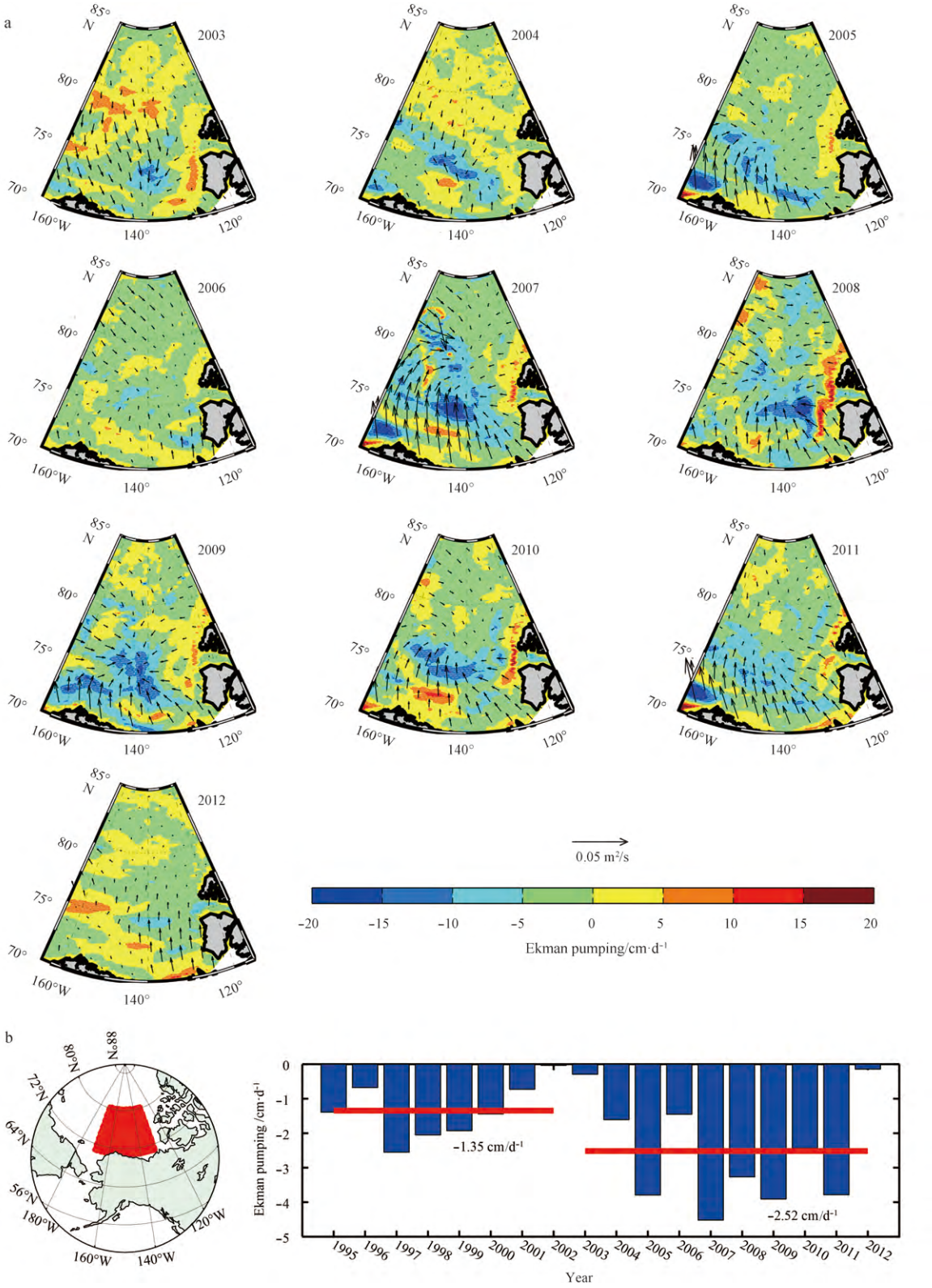

Fig. 3. Averaged (June to September) Ekman pumping. a. In the Canada Basin (the arrows show the Ekman transport) and b. in the BG region (70.5°–80.5°N, 130°–170°W).

The increasing freshwater content changes the baroclincity, further causes the change of the geostrophic current. The center of freshwater content is corresponding to the BG center as well as the dynamic height center (Fig. 6). The center of dynamic height was moving to the southwestern basin over time. The geostrophic current may drive the sea ice motion against the cyclonic wind in summer (Proshutinsky et al., 2002). The geostrophic current in 2000s showed a tremendous increase compared to the climato-

logy geostrophic current (Figs 6 and 1). Similar to the freshwater content, the geostrophic current was relatively stable in 2003–2006, but increased rapidly after 2007 (reaching the maximum in 2008) and decreased gradually after 2010. The strongest geostrophic current (crelative to 400×10^4 Pa) can be larger than 10 cm/s during 2008–2010 in anticyclonic circulation. The largest dynamic height (relative to 400×10^4 Pa) was about 0.65 gpm (geopotential meter) in 2003 and larger than 0.85 gpm in 2008. The horizontal gradient of dynamic height was becoming steep. The spin-up of BG and fresher upper ocean all contribute to much steeper bowl shape of BG in the upper ocean.

Mooring data indicate the Bering Strait throughflow increases

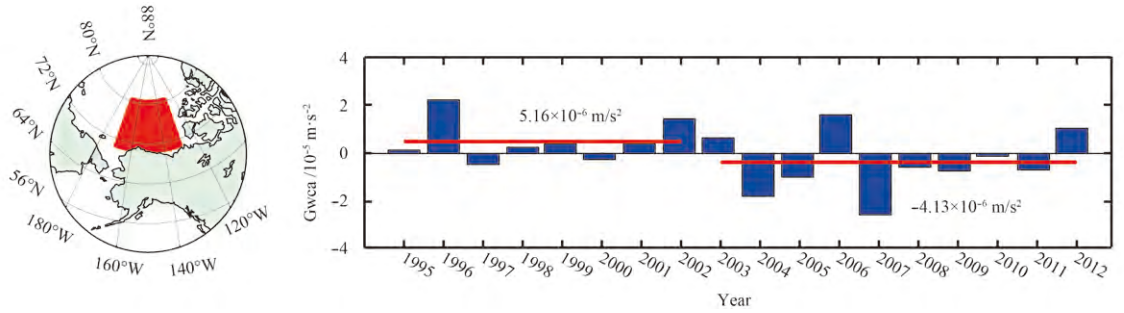

Fig. 4. Geostrophic wind curl anomaly (Gwca, 1995–2012, annual mean) in the BG region (70.5°–80.5°N, 130°–170°W).

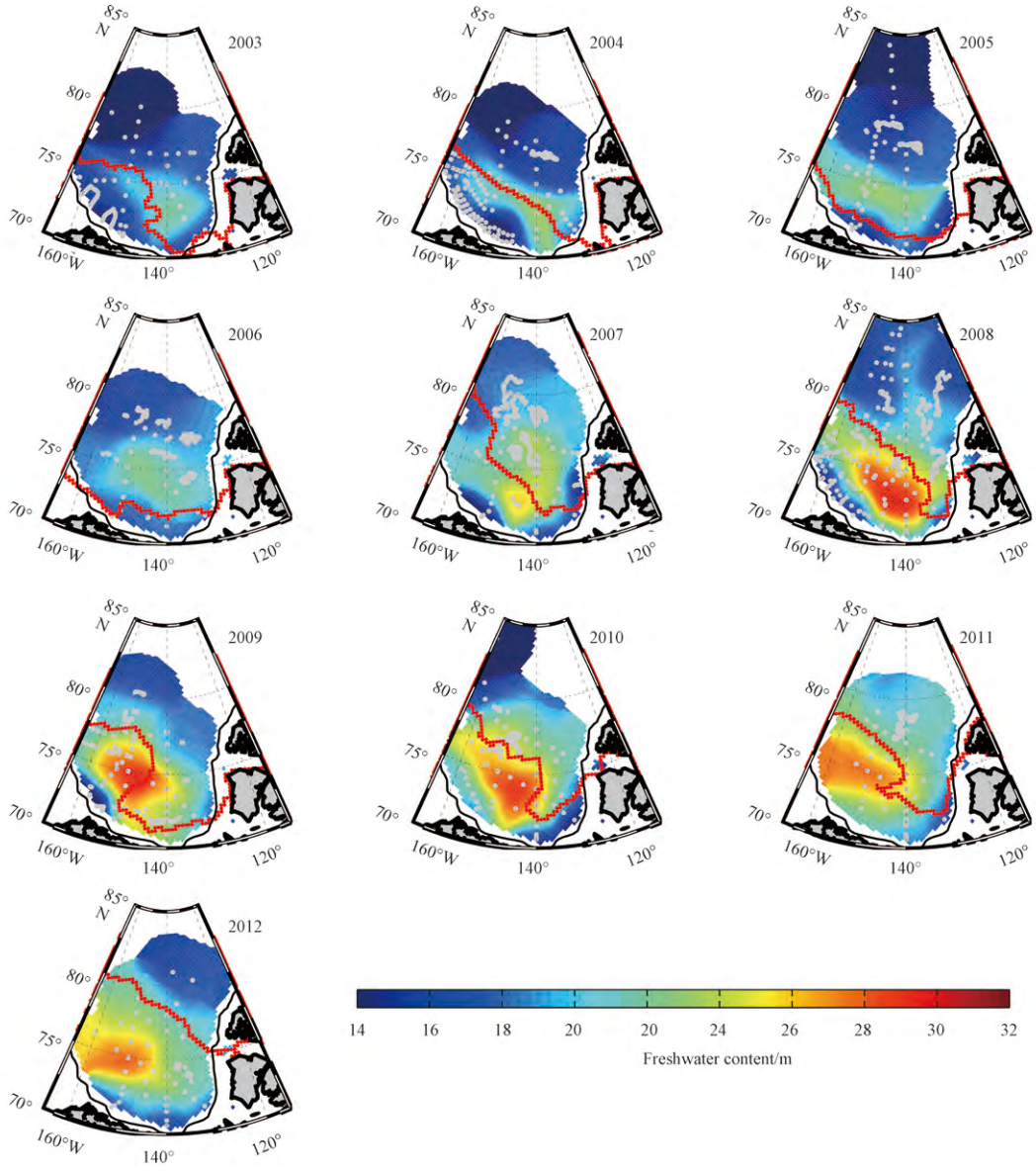

Fig. 5. The freshwater content relative to 34.8 isohaline. The thick red curves denote the September mean ice edge.

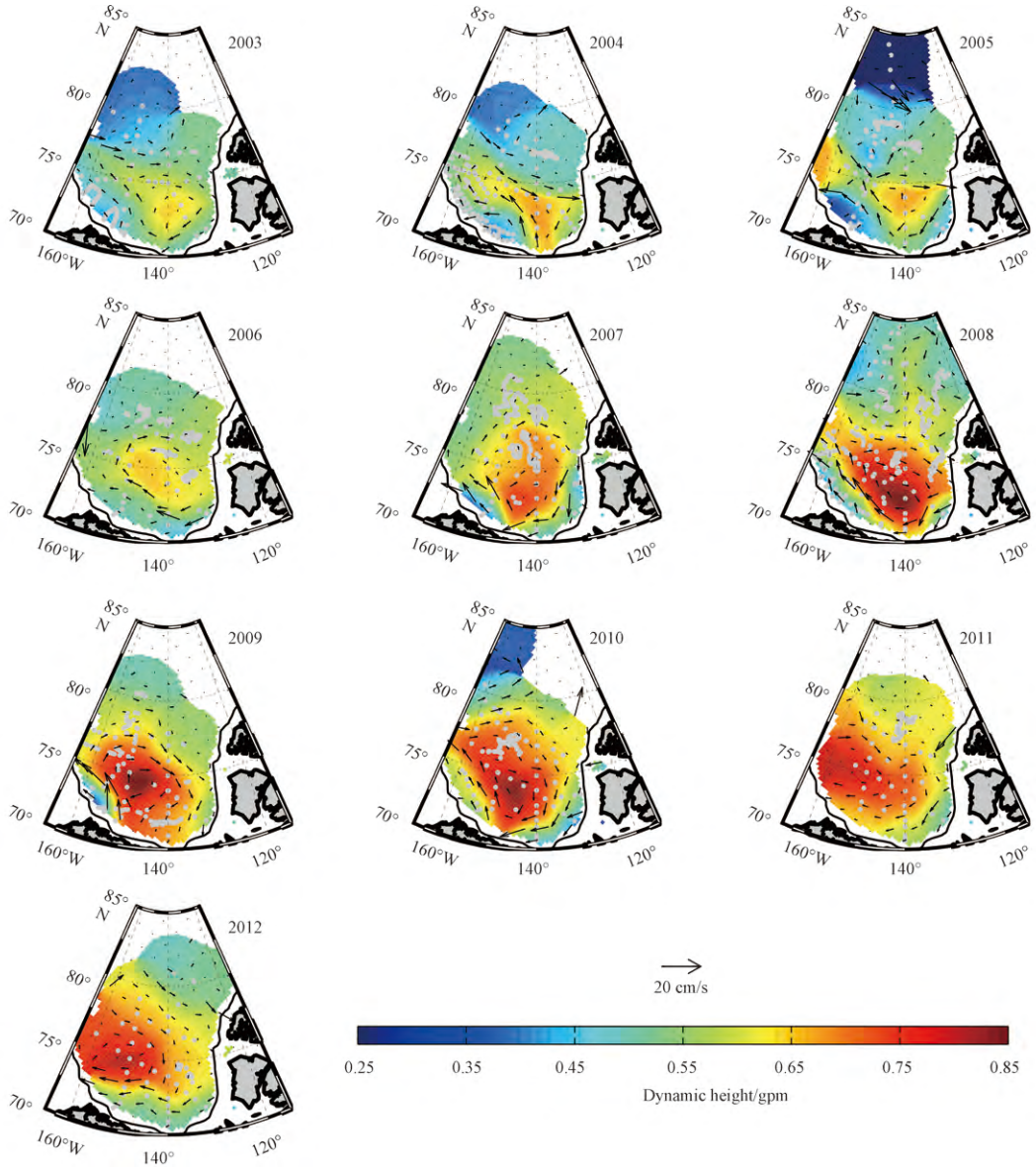

Fig. 6. Surface geostrophic current denoted by arrow heads and dynamic height denoted by colors (relative to 400 $\times 10^4$ Pa).

about 50% from 2001 (about 0.7×10^6 m^3/s) to 2011 (about 1.1×10^6 m^3/s) resulting in the heat and freshwater flux increases (Woodgate et al., 2012). However, the maximum temperature of PSW in the Canada Basin did not show a continue increasing trend (Fig. 7) The BG was stronger in 2005 (Fig. 3b) and one year later (2006) the temperature of the Pacific Summer Water (PSW, maximum temperature within the salinity range 31–33) reduced inside the BG (Fig. 7). When the BG became weaker in 2006, more PSW flowed into the BG center resulting in an anomalous high PSW temperature in 2007. There are other similar evidences happened in 2008 and 2009, such as the reduction of PSW temperature corresponding to the previous year's strong BG. The PSW temperature recovered to a relatively high value in 2011 as weaker BG appeared in 2010 summer.The BG was much weaker throughout the year in 2012 thus allowing more PSW to flow into the BG and return to a high PSW temperature inside the BG. In 2009 the region that outside the BG shows a high temperature-within the salinity range 28–30 while the PSW temperature reduced inside the BG. Two sources of water may make contribution to the high temperature outside BG, the relatively high NSTM and the shifting of PSW pathway from flowing to the Beaufort slope to the Northwind Ridge (McLaughlin et al., 2011). There are no water mass differences inside or outside BG essentially, but the intensity of BG would impact on the distribution of Pacific water in two ways. One is the Pacific water volume inside BG. The other is the water column properties through EP convergence. Most of the Pacific water flows into the basin in summer thus the intensity of summer BG determines the reservoir of Pacific water in the basin which may affect the maximum temperature of PSW in next year. What we need to notice is the distribution of PSW inside the BG was also related to the shifting position of the BG. During the later period of 2003–2012, the BG is shifting toward the Northwind Ridge.In a recent study, Timmermans et al. (2014) had shown that the Chuckchi Sea provided the subduction of PSW that flowed into the Canada Basin, and the Ekman transport convergence maintained the PSW ventilation of the halocline.

The seasonal deepening of NSTM is affected by turbulent diffusion over time (Zhao et al., 2003) and also the seasonal intensifying of Ekman Pumping (Jackson et al., 2010). We hypothesize that the role of turbulence may be small for the freshwater to develop deeper as the upper ocean becomes more stratified; instead it's the EP that determined it. The salinity of PSW inside the BG was reduced by about 1 during 2009–2012 compared to thoseprior to 2009.The fresher PSW may neither be the change of PSW upstream nor the shifting of PSW pathway. Instead, it may be due to the increasing salt diffusion from PSW to the fresher rWML (Jackson et al., 2011).

The isohaline of 33.1 could represent the Pacific Winter Water (PWW). The depth of 33.1 isohaline showed an increasing trend in 2003–2012 with the depth shallower than 150 m in 2003 and approaching 190 m in 2011 (Fig. 8). There are two mechanisms to explain the deepening of PWW, i.e., the increasing freshwater content and the dynamic effect of BG (McLaughlin and Carmack, 2010; Proshutinsky et al., 2009). The deepest PWW around the basin is corresponding to the location of maximum EP (Fig. 8a). The depth of PWW increased rapidly after 2007 with its deepest center toward the southwestern basin. What's more, the depth of PWW in the BG region is associated well with the intensity of BG (Figs 3b and 8b). The depth of PWW increased with the BG spin-up and decreased a little with the weaker BG in 2006, 2010 and 2012. It seems that the depth of PWW is synchronized with the intensity of EP to some extent.

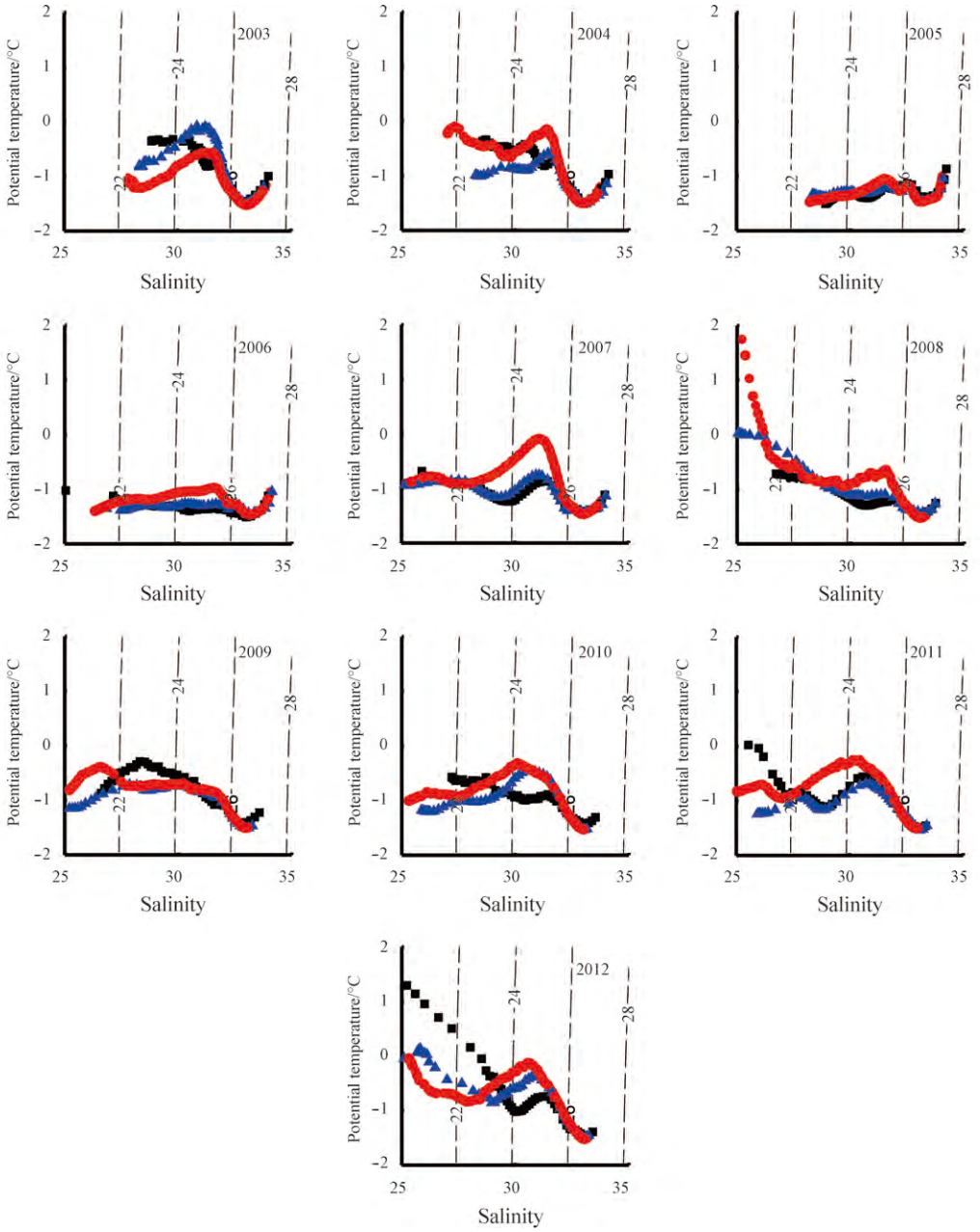

Fig. 7. *T-S* diagram of upper ocean (200 m) inside the BG (red dots), in the transition zone (blue triangles), outside the BG (black squares). The dash line shows the isopycnal.

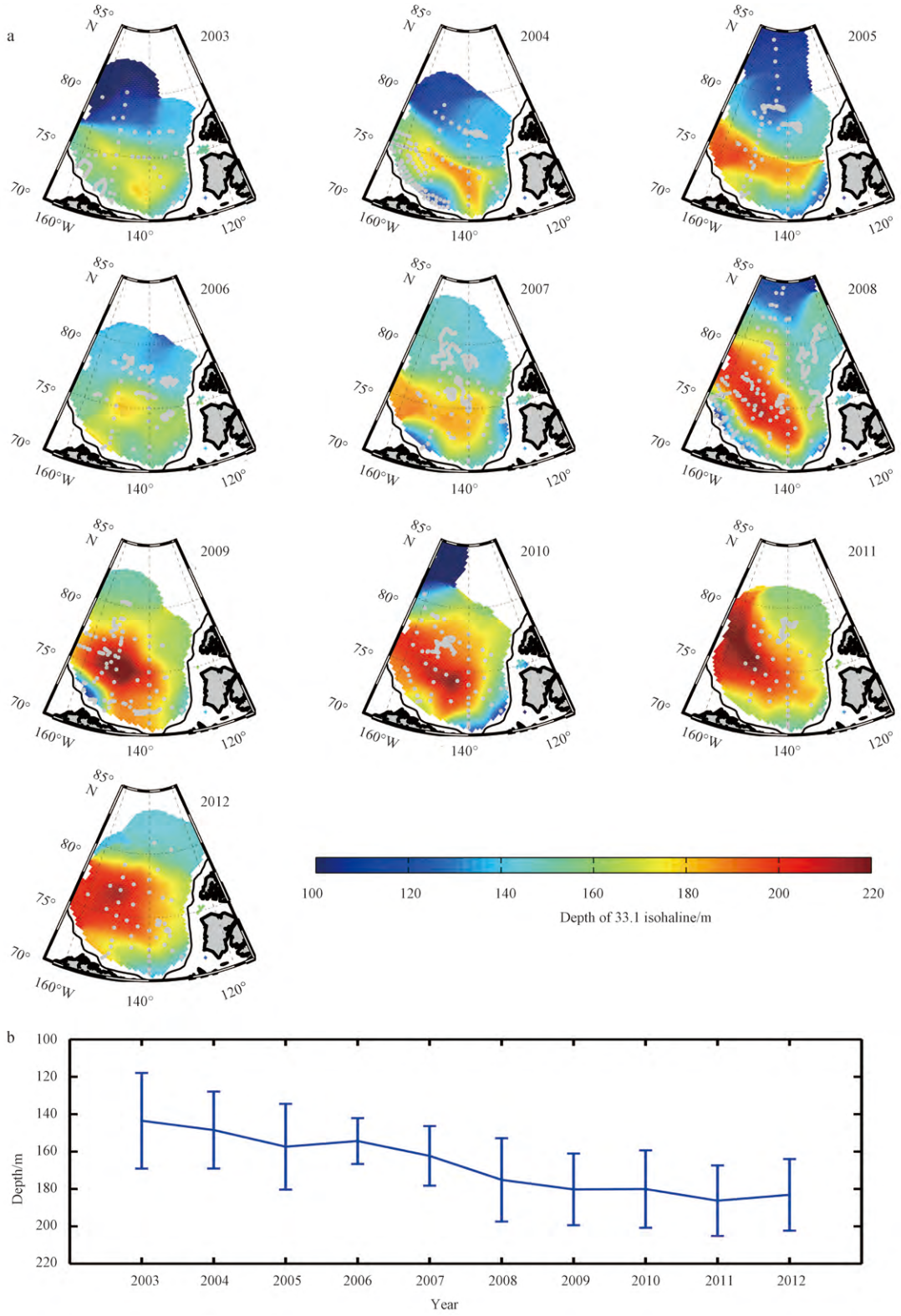

Fig. 8. Depth of 33.1 isohaline of Pacific Winter Water. a. Around the basin, and b. average depth of 33.1 isohaline of PWW in the above interpolating field of BG region (70.5°–80.5°N, 130°–170°W). The error bar represents the standard deviations of this isohaline depth for each year, derived from the original data with no spatial interpolation.

An interesting phenomenon is the area of deepest PWW is corresponding to the ice-free area (the red curves in the southwestern basin, shown in Figs 8a and 5). The shifting of EP center toward the southwestern basin may be related to the ice-free area which results in the area of the maximum depth of PWW.The intense EP means more surface water convergence and stronger downwelling that would affect the water column which is disadvantageous to the primary production. On the contrary, the up-

welling as compensation in the continental slope would bring more nutrients from deep water to the surfaces, which benefit the primary production (McLaughlin et al., 2010).

4.2 *Impact of BG on the Atlantic Water*

The Atlantic Water (AW) temperature reached its highest in 2003 and then gradually decreased from 2004 in the northwestern basin (the place where the AW flows into the basin through thermohaline intrusion, as indicated by McLaughlin et al., 2009) (Fig. 9a). The cooling process of AW is not attributed to more heat flux from AW to the upper ocean (the upward heat flux from AW is less than 1 W/m^2, Timmermans et al., 2008; Lique et al., 2014), instead, it's the result of inflow of relatively cold AW (Zhong and Zhao, 2014). Eddies are effective to enhance the vertical heat transfer (e.g., Lique et al., 2014), but we need more observations to inspect whether the numbers of eddies are increasing or not and its effect to the overall trend of AW variation. So far, the cooling trend during 2004–2012 in the northwestern basin is due to the inflow of relatively cold AW. There is an obvious "S" shape of AW anticyclonic intrusion in 2004–2007 under the influence of BG (McLaughlin et al., 2009). The AW deepened after 2007 as the result of the spin-up of BG, which enhanced negative surface stress curl, in a relatively stable AW temperature variation (Zhong and Zhao, 2014). The thermodynamic effect of relatively cold AW and dynamic effect of BG are the two mechanisms that contribute to the deepening of AW. Based on the regions that we classified (Fig. 2), Fig. 9b shows the depth variation of AW core in different regions (inside of BG, transition zone, outside of BG). The AW depth differences among the three regions increases as the BG spin-up which indicates enhanced negative surface stress curl. The standard deviationsof AW core depth inside the BG were larger when the BG spun up in 2008, 2009 and 2011, while smaller in 2010 and 2012 when the BG became weaker (refer to the errorbar in Fig. 9b). The depth of AW core became

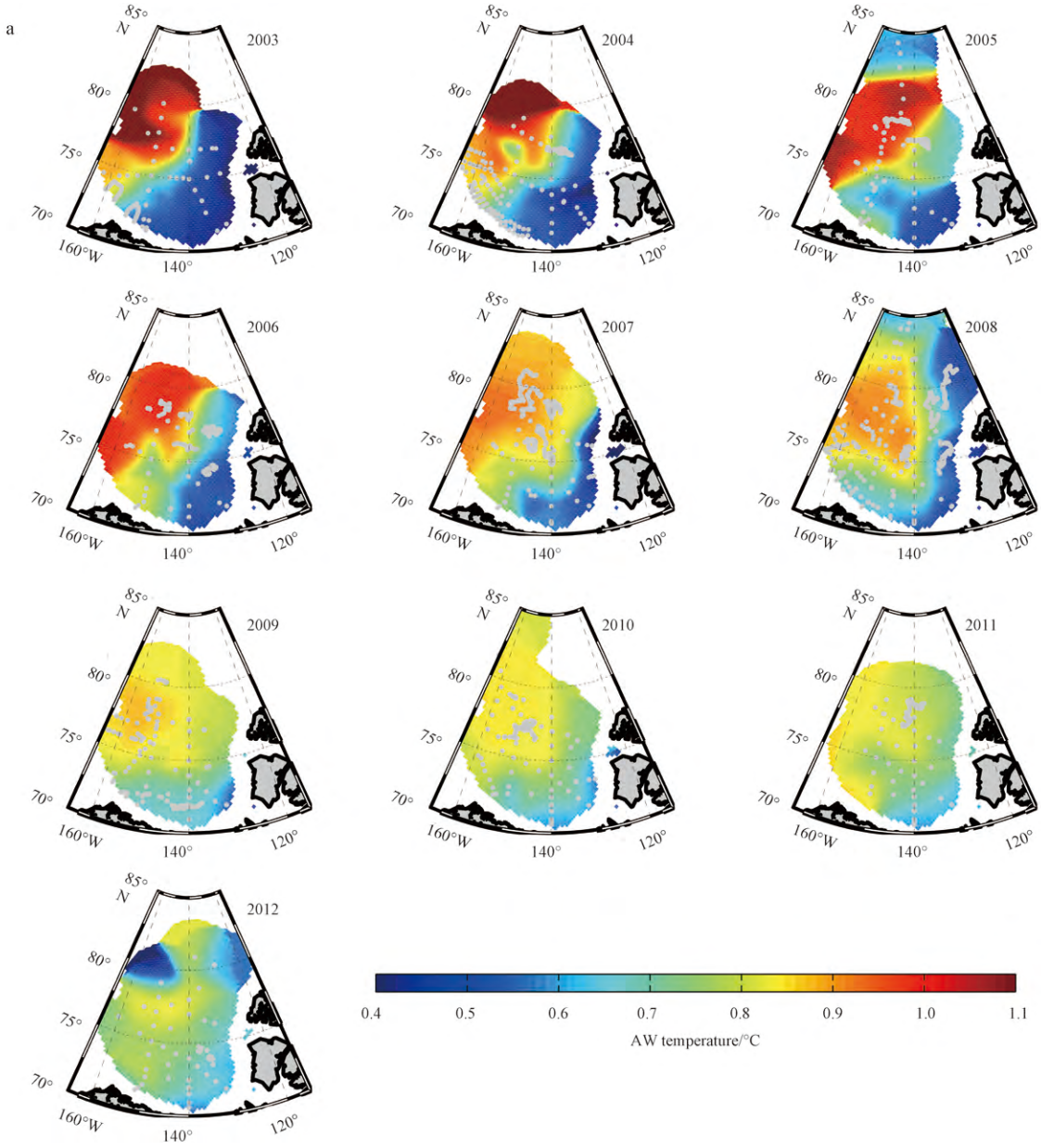

Fig. 9.

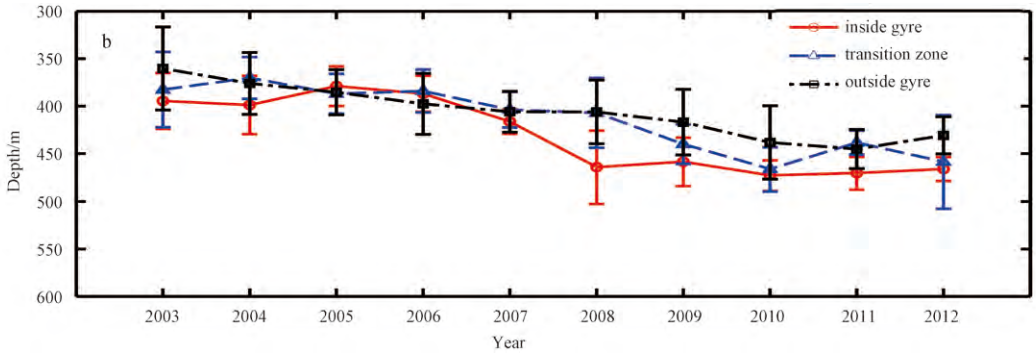

Fig. 9. The depth variation of Atlantic Water core. a. Around the basin (the values between stations are interpolated), and b. in the three regions related to the BG (inside of BG, transition zone and outside of BG). The error bar represents standard deviations of the AW core depth in the three separate regions for each year, which were derived from the original data with no spatial interpolation.

rather stable during 2008–2012 (about 470 m). The increasing freshwater content has changed the properties of water column thus the change of dynamic height which influenced the depth of AW core. Based on a $2^{1/2}$-layer (reduced-gravity) model, Zhong and Zhao (2014) estimated that the enhanced negative surface stress curl could increase the AW core depth into about 60 m.

The depth of AW core in the inside of BG is larger than those observed in the transition zone and outside of BG at most of the time, which indicates the dynamic impacts of BG. The 2007 seems to be a transition year of AW core depth from 400–410 m before 2007 to about 470 m after 2007. As more relatively cold AW flowed into the basin through Northwind Ridge, there appeared small difference of the AW core depths between the regions that inside of BG and the transition zone, but big difference compared to the outside of BG (Fig. 9a). The spin-up of BG inside the basin would increase the upwelling along the Beaufort slope region (no double-diffusive staircase region) which may cause more vertical heat transfer from the AW to the upper ocean (Timmermans et al., 2008; Zhao and Zhao, 2011).

5 Discussion and conclusions

The Canada Basin is experiencing a rapid decline of sea ice in recent years with most of the multi-year sea ice replaced by first-year sea ice (Kwok et al., 2009; Hutchings and Rigor, 2012). More ice-free area appears in summer. The retreat of sea ice intensified the air-sea exchange which would change the environmental background by increasing turbulent mixing (Rainville et al., 2011).

The upper ocean shows an obvious warming trend (Steele et al., 2008; Zhong and Zhao, 2011) and increasing freshwater content (Proshutinsky et al., 2009; Rabe et al., 2014). The freshwater content in the Canada Basin is about 22 m in 2003–2006 and increased to about 28 m in 2007–2010 and then gradually decreased. The increasing freshwater content indicates the upper ocean becomes more stratified. The dynamic heights (relative to 400×10^4 Pa) in the Canada Basin had changed from the values smaller than 0.65 gpm (geopotential meter) in 2003 to those larger than 0.85 gpm in 2008 which resulted in the increasing of geostrophic current. The BG was spinning up in recent years with its center moving toward the southwestern basin which may be related to the dramatic decline of sea ice there.

The direct impact of BG to the upper ocean is deepening the PWW by accumulating the freshwater while the indirect impact of BG is deepening the AW by changing the dynamic properties of water column. The intensity of Beaufort Gyre controls the distribution of PSW in the Canada Basin. The maximum temperature of PSW was reduced or even disappeared in 2005 and 2009 in the central basin, which was the effect of stronger BG. The downwelling velocity (absolute value) in the BG region had been generally larger than 2 cm/d after 2003 (absolute value>4 cm/d in 2007 and <1 cm/d in 2012). Instead of downwelling, most of the basin was dominated by upwelling in 2012 and there was a strong northward Ekman transport in the basin which would benefit the release of freshwater that had resided in the basin for years. The intensity of BG is synchronized with the depth variation of PWW. The deepened AW core is the result of BG spin-up when the temperature of AW was in a relatively stable period. The depth of AW core changed from 400–410 m before 2007 to about 470 m after 2007. The BG variation is becoming more and more important in regulating the changes of the upper ocean. More observations are needed in order to better understand and predict the changes in the upper ocean.

Acknowledgements

We would like to express our high respects to the scientists and technicians at WHOI, DFO, CHINARE, JAMSTEC, SBI and Oden who carried out the field expeditions and shared the data with us in this study. The comments and suggestions from two anonymous reviewers have greatly improved the manuscript.

References

Aagaard K, Carmack E C. 1989. The role of sea ice and freshwater in the Arctic circulation. J Geophys Res, 94(C10): 14485–14498

Aagaard K, Swift J H, Carmack E C. 1985. Thermohaline circulation in the Arctic Mediterranean seas. J Geophys Res, 90(C3): 4833–4846

Asplin M G, Lukovich J V, Barber D G. 2009. Atmospheric forcing of the Beaufort Sea ice gyre: Surface pressure climatology and sea ice motion. J Geophys Res, 114: C00A06

Comiso J C. 2000. Bootstrap sea ice concentrations from nimbus-7 SMMR and DMSP SSM/I-SSMIS. Version 2. Boulder, Colorado USA: NASA DAAC at the National Snow and Ice Data Center

Comiso J C, Parkinson C L, Gersten R, et al. 2008. Accelerated decline in the Arctic sea ice cover. Geophys Res Lett, 35(1): L01703

Curry B, Lee C M, Petrie B, et al. 2014. Multi-year volume, liquid freshwater, and sea ice transports through Davis Strait, 2004–10. J Phys Oceanogr, 44(4): 1244–1266

De Steur L, Steele M, Hansen E, et al. 2013. Hydrographic changes in the Lincoln Sea in the Arctic Ocean with focus on an upper oceanfreshwater anomaly between 2007 and 2010. J Geophys Res Oceans, 118(9): 4699–4715

Dickson R, Meincke J, Malmberg S A, et al. 1988. The "great salinity anomaly" in the northern North Atlantic 1968–1982. Prog Oceanogr, 20(2): 103–151

Fowler C, Emery W, Tschudi M. 2013. Polar pathfinder daily 25 km EASE-Grid sea ice motion vectors, Version 2. Boulder, Colorado USA: NASA DAAC at the National Snow and Ice Data Center

Giles K A, Laxon S W, Ridout A L, et al. 2012. Western Arctic Ocean freshwater storage increased by wind-driven spin-up of the Beaufort Gyre. Nat Geosci, 5(3): 194–197

Hutchings J K, Rigor I G. 2012. Role of ice dynamics in anomalous ice conditions in the Beaufort Sea during 2006 and 2007. J Geophys Res, 117(C8): C00E04

Itoh M, Shimada K, Kamoshida T, et al. 2012. Interannual variability of Pacific Winter Water inflow through Barrow Canyon from 2000 to 2006. J Oceanogr, 68(4): 575–592

Jackson J M, Allen S E, McLaughlin F A, et al. 2011. Changes to the near-surface waters in the Canada Basin, Arctic Ocean from 1993–2009: A basin in transition. J Geophys Res, 116: C10008

Jackson J M, Carmack E C, McLaughlin F A, et al. 2010. Identification, characterization, and change of the nearsurface temperature maximum in the Canada Basin, 1993–2008. J Geophys Res, 115(C5): C05021

Kalnay E, Kanamitsu M, Kistler R, et al. 1996. The NCEP/NCAR 40-year reanalysis project. Bull Am Meteorol Soc, 77(3): 437–471

Karlqvist A. 2005. Cruise report: ODEN05 (updatedFEB 2010). Stockholm: The Swedish Polar Research Secretariat, 27

Kwok R, Cunningham G F, Wensnahan M, et al. 2009. Thinning and volume loss of the Arctic Ocean sea ice cover: 2003–2008. J Geophys Res, 114(C7): C07005

Lique C, Guthrie J D, Steele M, et al. 2014. Diffusive vertical heat flux in the Canada Basin of the Arctic Ocean inferred from moored instruments. J Geophys Res, 119(1): 496–508

McLaughlin F A, Carmack E C. 2010. Deepening of the nutricline and chlorophyll maximum in the Canada Basin interior, 2003–2009. Geophys Res Lett, 37(24): L24602

McLaughlin F A, Carmack E C, Proshutinsky A, et al. 2011. The rapid response of the Canada Basin to climate forcing: From bellwether to alarm bells. Oceanography, 24(3): 146–159

McLaughlin F A, Carmack E C, Williams W J, et al. 2009. Joint effects of boundary currents, thermohaline intrusions and gyre circulation on the recent warming of Atlantic Water in the Canada Basin: 1993–2007. J Geophys Res, 114(C1): C00A12

McLaughlin F, Carmack E C, Zimmerman S, et al. 2008. Physical and chemical data from the Canada Basin, August, 2004. Sidney, BC: Fisheries and Oceans, Science Branch, Pacific Region, Institute of Ocean Sciences, 140: 185

McPhee M G. 2013. Intensification of geostrophic currents in the Canada Basin, Arctic Ocean. J Climate, 26(10): 3130–3138

McPhee M G, Proshutinsky A, Morison J H, et al. 2009. Rapid change in freshwater content of the Arctic Ocean. Geophys Res Lett, 36(10): L10602

Moore G W K. 2012. Decadal variability and a recent amplification of the summer Beaufort Sea High. Geophys Res Lett, 39(10): L10807

Morison J, Kwok R, Peralta-Ferriz C, et al. 2012. Changing Arctic Ocean freshwater pathways. Nature, 481(7379): 66–70

Overland J E, Wang Muyin. 2010. Large-scale atmospheric circulation changes are associated with the recent loss of Arctic sea ice. Tellus A, 62(1): 1–9

Polyakov I V, Alexeev G V, Timokhov L A, et al. 2004. Variability of the intermediate Atlantic water of the Arctic Ocean over the last 100 years. J Clim,17(23): 4485–4497

Proshutinsky A Y, Bourke R H, McLaughlin F A. 2002. The role of the Beaufort Gyre in Arctic climate variability: Seasonal to decadal climate scales. Geophys Res Lett, 29(23): 15–1–15–4

Proshutinsky A, Dukhovskoy D, Timmermans M-L, et al. 2013. Arctic circulation regimes and their transformations under the influence of climate change. Geophys Res Abstr, 15: EGU2013-1581

Proshutinsky A Y, Johnson M A. 1997. Two circulation regimes of the wind-driven Arctic Ocean. J Geophys Res, 102(C6): 12493–12514

Proshutinsky A, Krishfield R, Timmermans M-L, et al. 2009. Beaufort Gyre freshwater reservoir: State and variability from observations. J Geophys Res, 114(C1): C00A10

Rabe B, Karcher M, Kauker F, et al. 2014. Arctic Ocean basin liquid-freshwater storage trend 1992–2012. Geophys Res Lett, 41(3): 961–968

Rabe B, Karcher M, Schaueret U, et al. 2011. Anassessment of Arctic Ocean freshwater content changes from the 1990s to the 2006–2008 period. Deep-Sea Res Pt I, 58(2): 173–185

Rainville L, Lee C M, Woodgate R A. 2011. Impact of wind-driven mixing in the Arctic Ocean. Oceanography, 24(3): 136–145

Rampal P, Weiss J, Marsan D. 2009. Positive trend in the mean speed and deformation rate of Arctic sea ice, 1979–2007. J Geophys Res, 114(C5): C05013

Rennermalm A K, Wood E F, Déry S J, et al. 2006. Sensitivity of the thermohaline circulation to Arctic Ocean runoff. Geophys Res Lett, 33(12): L12703

Rigor I G, Wallace J M, Colony R L. 2002. Response of Sea Ice to the Arctic Oscillation. J Clim, 15(18): 2648–2663

Shimada K, Nishino S, Itoh M. 2004. R/V Mirai cruise report MR04–05. Yokosuka, Japan: Japan Agency for Marine-Earth Science and Technology

Steele M, Ermold W, Zhang J. 2008. Arctic Ocean surface warming trends over the past 100 years. Geophys Res Lett, 35(2): L02614

Swift J H, Codispoti L. 2003. Update 2010, SBI 2003 cruise report of R/V Nathaniel B. Palmer. La Jolla: Scripps Institution of Oceanography, 129

Thompson D W J, Wallace J M. 1998. The Arctic oscillation signature in the wintertime geopotential height and temperature fields. Geophys Res Lett, 25(9): 1297–1300

Timmermans M-L, Proshutinsky A, Golubeva E, et al. 2014. Mechanisms of pacific summerwater variability in the Arctic's Central-Canada Basin. J Geophys Res, 119(11): 7523–7548

Timmermans M-L, Proshutinsky A, Krishfield R A, et al. 2011. Surface freshening in the Arctic Ocean's Eurasian Basin: An apparent consequence of recent change in the wind-driven circulation. J Geophys Res, 116(C8): C00D03

Timmermans M-L, Toole J, Krishfield R, et al. 2008. Ice-Tethered Profiler observations of the double diffusive staircase in the Canada Basin thermocline. J Geophys Res, 113(C1): C00A02

Tsamados M, Feltham D L, Schroeder D, et al. 2014. Impact of variable atmospheric and oceanic form drag on simulations of Arctic sea ice. J Phys Oceanogr, 44(5): 1329–1353

Wang Jia, Zhang Jinlun, Watanabe E, et al. 2009. Is the Dipole Anomaly a major driver to record lows in Arctic summer sea ice extent?. Geophys Res Lett, 36(5): L05706

Woodgate R A, Weingartner T J, Lindsay R. 2012. Observed increases in Bering Strait oceanic fluxes from the Pacific to the Arctic from 2001 to 2011 and their impacts on the Arctic Ocean water column. Geophys Res Lett, 39(24): L24603

Yamamoto-Kawai M, McLaughlin F A, Carmack E C, et al. 2009. Surface freshening of the Canada Basin, 2003–2007: River runoff versus sea ice meltwater. J Geophys Res, 114(C1): C00A05

Yang Jiayan. 2009. Seasonal and interannual variability of downwelling in the Beaufort Sea. J Geophys Res, 114(C1): C00A14

Yang Jiayan, Proshutinsky A. 2013. Atmospheric forcing of the freshwater content in the Beaufort Gyre. Vienna, Austria: EGU General Assembly, EGU2013–11434

Zhao Jinping, Shi Jiuxin, Jiao Yutian. 2003. Temperature and salinity structure in summer marginal ice zone of Arctic Ocean and an analytical study on theirthermodynamics. Oceanologiaet Limnologia Sini (in Chinese), 34(4): 375–388

Zhao Qian, Zhao Jinping. 2011. Distribution of double-diffusive staircase structure and heat flux in the Canada Basin. Adv Earth Sci (in Chinese), 26(2): 193–201

Zhong Wenli, Zhao Jinping. 2011. Variation of upper-ocean heat content in the Canada Basin in summers of 2003 and 2008. Adv Polar Sci, 22(4): 235–245

Zhong Wenli, Zhao Jinping. 2014. Deepening of the Atlantic Water Core in the Canada Basin in 2003–11. J Phys Oceanogr, 44(9): 2353–2369

Appendix:

The Gaussian interpolation method we used here is a iterate correction method. The influence radius we used here is 300 km.

$$F_0(i,j) = \frac{\sum_{k=1}^{K} F(k) W_0(i,j,k)}{\sum_{k=1}^{K} W_0(i,j,k)}, \tag{A1}$$

$$W_0(i,j,k) = \exp\left(\frac{-r_{i,j,k}^2}{4a}\right), \tag{A2}$$

where $K(k)$ is the original CTD stations, $F_0(i, j)$ is the interpolated points, $r_{i,j,k}$ is the distance between the new grid points to the CTD cast stations, K is the total number of stations in the radius of influence, "a" is an constant.

Used $K_0(k)$ represents the interpolated point back to the CTD station $K(k)$, we then estimate the interpolation errors as $F_D(k) = F(k) - F_0(k)$. The errors of CTD stations are used to interpolate back to the new grid using Eqs (A1) and (A2) again. And we have $F_D(i, j)$ as the errors for each data point in the new grid.

Finally, we have the interpolation data in the new grid as $F(i,j) = F_0(i,j) + F_D(i,j)$. For more accuracy estimate of the statistical mapping error, readers can refer to Rabe et al. (2011).